Synthesis and Characterization of Nano-Hydroxyapatite/mPEG-*b*-PCL Composite Coating on Nitinol Alloy

Mohamadreza Etminanfar[*,1], *Jafar Khalil-Allafi*[1], *Kiyumars Jalili*[2]

[1]*Research Center for Advanced Materials, Faculty of Materials Engineering, Sahand University of Technology, Tabriz, Iran.*

[2]*Institute of Polymeric Materials, Faculty of Polymer Engineering, Sahand University of Technology, Tabriz, Iran.*

ABSTRACT

In this study the bioactivity of hydroxyapatite/poly(ε-caprolactone)–poly(ethylene glycol) bilayer coatings on Nitinol superelastic alloy was investigated. The surface of Nitinol alloy was activated by a thermo-chemical treatment and hydroxyapatite coating was electrodeposited on the alloy, followed by applying the polymer coating. The surface morphology of coatings was studied using FE-SEM and SEM. The data revealed that the hydroxyapatite coating is composed of one-dimensional nano sized flakes and the polymer coating is uniformly covered the sublayer. Also, High resolution TEM studies on the hydroxyapatite samples revealed that each flake contains nano-crystalline grains with a diameter of about 15 nm. The hydroxyapatite monolayer coating was rapidly covered by calcium phosphate crystals (Ca/P=1.7) after immersion in simulated body fluid confirming the bioactivity of the nanostructured flakes. However, the flakes were weak against applied external forces because of their ultra-fine thickness. Scratch test was applied on hydroxyapatite/polymer coating to evaluate delamination of the coating from substrate. It was shown that, the polymer coating has a great influence on toughening the hydroxyapatite coating. To assess the degradation effect of the polymer layer on hydroxyapatite coating, samples were immersed in phosphate-buffered saline at 37 °C. SEM studies on the samples revealed that the beneath layer of hydroxyapatite appears after 72 h without any visible change in morphology. It seems that, application of a biodegradable polymer film on the nanostructured hydroxyapatite coating is a good way to support the coating during implantation processes.

Keywords: *Nitinol; HA film; Nano-sized; mPEG-b-PCL; biodegradable.*

1. Introduction

NiTi alloys are one of the important metallic biomaterials due to their unique properties such as superelasticity and shape memory effect [1, 2]. There are some problems in the application of these alloys as implants especially because of the Ni release and the bio inert surface. The bio inert surface leads to the formation of a nonadherent layer at the surface of implants and failing of the implantation [3-6].

To achieve best results after implantation, the biomaterial must closely resemble natural tissue structure. Human bone is a composite of nano-sized Ca-P crystals and natural polymers of body like collagen that have supporting rule in the tissue [7-9]. Bone tissue minerals have a plate like morphology in which the thickness of the platelets ranges from 2 to 7 nm, the length from 15 to 200 nm and the width from 10 to 80

nm. The main component of the organic matrix of bone is type I collagen which is a large fibrous protein. Typically, the protein matrix is tough but not very stiff while the minerals are stiff but not very tough. The influence of organic components on the mechanical properties of bone tissue can be recognized by comparing the elastic modulus and fracture strain of bone constituents in which these values for minerals are 135 GPa and 0.1%, and for type I collagen 1 GPa and 10%, respectively. In the composite tissue of bone the values are10–25 GPa and 1–1.5%, respectively [10].

It was shown that in synthetic scaffolds, nanosized HA increased protein adsorption and cell adhesion to the biomaterial and improved the mechanical and biological properties at the same time. However, it must be considered that nano sized plates of hydroxyapatite cannot be completely survived during the implantation process [9, 11].

The brittleness of the nanostructured HA coating is expected to be overcome by using a polymer top layer coating. Biodegradable polymers can be gradually removed in human body making the opportunity of substitution natural body components on the surface of HA coating. Moreover, drugs may be efficiently loaded on the coating by applying the polymer film [12].

Different biodegradable polymers can be used to control properties such as biocompatibility, rate of degradability and mechanical properties, making the materials suitable for use in a wide range of biomedical applications.

Poly (ε-caprolactone) (PCL) is synthetic polyester exhibiting a low glass transition temperature of around 60 ˚C which provides a rubbery characteristic in the material. PCL undergoes auto-catalyzed bulk hydrolysis. The semi-crystalline nature of the polymer extends its resorption time to over 2 years since the close packed macromolecular arrays retard fluid ingress. Copolymerization of caprolactone with poly(ethylene glycol) (PEG) has been investigated to increase degradation rates and improve processability [13].

Despite the progress made towards the application of nanostructured bioactive coatings on metallic implants, the stability of coatings during implantation is one of the most important issues in this field. In this study, a biodegradable mPEG-*b*-PCL well defined diblock copolymer top layer coating is applied on HA coating and the bioactivity and stability of nanostructured HA coatings is evaluated through in-vitro tests.

2. Experimental details
2.1. Preparation of specimens

In this work, NiTi rod with nominal composition of 50.9% Ni was used as substrates. The rods with the diameter of 13mm were sliced into 1mm disks. The surface of samples was abraded with different grades of SiC papers from P80 to P600 grit and then was etched in an acid solution of 1 HF-4 HNO_3-5 H_2O for 4 min, and finally was soaked in distilled boiling water for 20 min. After each step, specimens were cleaned in acetone and then rinsed with deionized water. For the heat treatment process, the specimens were encapsulated in a glass tube after purging and vacuuming the high purity Ar gas inside the tubes for several times. The heat treatment carried out at 470 ˚C for 30 min.

2.2. Electrochemical deposition

The electrodeposition was performed in an individual cell using a regular two electrode configuration in which NiTi alloy served as the cathode and a platinum mesh act as the anode. The distance between the anode and the cathode was fixed at 20 mm. An electrolyte solution of 0.0084M $Ca(NO_3)_2.4H_2O$, 0.005M $NH_4H_2PO_4$, 0.1M $NaNO_3$, and 6 ml/l H_2O_2 was prepared and used for the electrodeposition. The pH of the electrolyte was 6.0 and the temperature of the electrolyte was maintained at 65±1°C using Bain-Marie method. The deposition was carried out using a bipolar pulsed current with the direct current (ON) time of 1s and the reverse current time of 2s. The direct and reverse pulse current densities were -3.0 and 0.1 mA/cm², respectively. An inert gas was purging during electrodeposition and mechanical stirring of the electrolyte was controlled at a speed of 150 rpm.

2.3. Synthesis of mPEG-b-PCL Diblock Copolymer

A typical procedure of ring opening polymerization was used to synthesize the copolymer using substituted εcaprolactone (ε-CL) monomer with $[M_0]/[I_0]$=95 and polyethylene glycol monomethyl ether (mPEG) (MW = 1000) as initiator (for polymer mPEG-*b*-PCL_{96}). Under a N_2 atmosphere, a solution of PEG (28.0 mg, 0.0145 mmol) was taken in a flame-dried Schlenk tube, and dry toluene (1.5 mL) was added. To this mixture, $Sn(Oct)_2$ (2.8 mg, 0.00725 mmol) was added, and the content was stirred at room temperature (r.t) for 20 min under nitrogen purge. The ε-CL (0.5 g, 1.64 mmol) was added to the mixture, and the polymerization

mixture was proceeded at r.t. for 30 min. The reaction tube was immersed in preheated oil bath at 130 °C, and the polymerization was continued for 2 days with constant stirring. The polymerization mixture was precipitated in methanol. The polymer was redissolved in Tetrahydrofuran (THF) and precipitated again in methanol. The purification was done at least twice to obtain highly pure polymer.

1H NMR (400 MHz, CDCl$_3$)

δ ppm: 4.13 (s, 2H), 3.64 (s, 3.8 H), 3.45 (s, 1H), 3.38 (s, 1H), 2.44 (t, 2H), 2.35 (t, 2H), 1.93−1.81 (m, 2H), 1.81−1.67 (m, 4H), 1.44 (s, 9H, t-butyl).

13C NMR (100 MHz, CDCl$_3$)

δ ppm: 173.63, 170.81, 80.72, 75.58, 70.68, 65.13, 61.47, 36.60, 33.04, 29.81, 28.86, and 28.22. GPC molecular weights: Mn = 4560, Mw = 5700, and PDI = 1.25.

To deposit the polymer top layer coating, the synthesized polymer was dissolved in ethanol (1 mg/ml) and the solution was drop casted on HA coated samples and then allowed to dry at room temperature. The ratio between volume of the drop casted solution and the apparent surface area of HA coating was ~0.1.

2.4. Characterization of modified samples and coatings

The surface morphology of the deposited films was examined by a Cam Scan MV2300-Czech scanning electron microscope (SEM) equipped with an energy dispersive spectroscopy (EDS) analyzer and FEI-Quanta 400 FE6–Netherland field emission SEM. The operating voltage in both microscopes was 20.0 kV.

The high resolution transmission electron microscopy (HRTEM) images were collected using Tecnai G2 F20 (USA) system, operating at 200 kV. For this purpose, the scrapped samples were transferred to vials and absolute ethanol added. After ultrasonic operation, the well-dispersed samples were drop-casted onto copper grids for TEM analysis.

The bioactivity of the Ca-P coating was investigated by immersing the coated sample in simulated body fluid (SBF) for 7 days at 37 °C. The samples were freely suspended in a volume of SBF solution approximately corresponding to a surface to volume ratio S/V = 0.05 cm^{-1}. The SBF was prepared according to Kokubo's instruction [14] and it was buffered to pH 7.4 at 37 °C by adding 1 M HCl and Tris (hydroxymethyl aminomethane).

In order to stabilize the ion concentration and the pH value of SBF, the solution was refreshed each two days.

3. Results and discussion

The surface morphology of the pulse deposited HA coating is depicted in Fig. 1. The coating is composed of ultrafine and uniform flakes and the thickness analysis of plates revealed that the data are in the range of 10-90 nm. Although the size of flakes is somewhat larger than that of the bone minerals, the morphology is almost the same. It can be seen in Fig. 1 that there is almost a same growth direction for the flakes of the coating related to the cathode surface. This morphology is nearly resemble to the bone minerals accommodation. It must be considered that our previous results revealed that the coating is composed of HA and other Ca-P phases are rare in the film [15]. So, the structure of the deposited film is also near to that of the bone minerals.

The high resolution TEM image of the electrodeposited coating is shown in Fig. 2. This image is taken perpendicular to one of the flakes of the coating. A crystalline grain with a diameter of ~15 nm can be detected in the figure. Also, some irregular regions at the intersection of two adjacent grains can be seen which are labeled with arrows. This observation revealed that there are thin regions inside the flakes which have different crystalline state or structure. Possibly, the observed structure is formed during the repeated deposition and dissolution processes of the applied bipolar pulse current.

Detailed analyzing on the crystalline regions of Fig. 2 reveals two different kinds of atomic arrangement. HA can crystallize in two forms
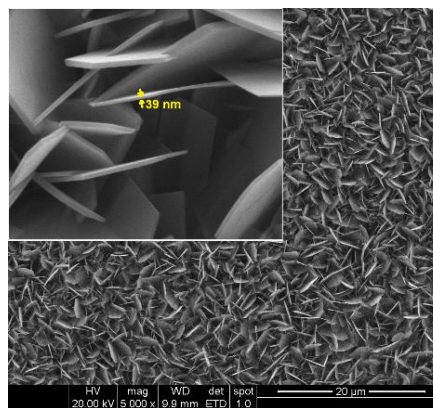
Fig. 1- FE-SEM micrographs of the pulse deposited HA coating.

of hexagonal and monoclinic. It was shown that the zigzag atomic arrangement can be related to the monoclinic HA [16]. The major difference between the monoclinic and the hexagonal HA is the orientations of the hydroxyl groups. In the hexagonal phase, the hydroxyl groups place along the c-axis and the adjacent groups point in opposite directions. The hydroxide ions in the monoclinic phase are pointed in the same direction in a given column, and the direction reverses in the next column; accordingly the b-axis is doubled in comparison with that of the hexagonal phase [17]. The monoclinic phase is the most ordered and structurally stable form of HA. Based on the theoretical results, the monoclinic phase of HA energetically is more favorable phase than the hexagonal one [18]. On the other hand, considering the kinetic factor, the formation of hexagonal phase in ordinary conditions is more favorable compared to the monoclinic phase. Some parameters like high temperature and high pH can result in the formation of monoclinic phase [19, 20]. Supplying an insufficient amount of hydroxyl groups during the deposition can result in disturbing the order of hydroxyl groups and formation of hexagonal phase instead of monoclinic phase. It seems that in our case the bipolar pulsed current produces a step by step deposition condition and supplies more hydroxyl groups than DC electrodeposition which increase the opportunity of the monoclinic phase formation [21].

The ability of apatite formation, which reveals the bioactivity of materials, can be estimated using immersion of samples in SBF [22]. The surface morphology of the HA coated sample after immersion in SBF is depicted in Fig. 3. The

EDS analysis of the coating reveled that Ca/P ratio in the coating is 1.7 which is near to that of the pure hydroxyapatite crystal. It can be seen that the sample is completely covered by HA crystals after immersion in SBF for one week which shows a good bioactivity of the coating in physiological mediums. This result confirms that the synthesized coating can be rapidly connected with surrounding tissues after implantation which increase the chance of sound implantation.

Although the HA coatings revealed a good bioactivity due to its composition and ultra-fine structure, the coating was weak against shear stress. Fig. 4 shows HA coating with damaged surface as a result of external stresses. This limitation can result in decreasing the bioactivity or non-uniform surface of the coated alloy after the packing and implantation process.
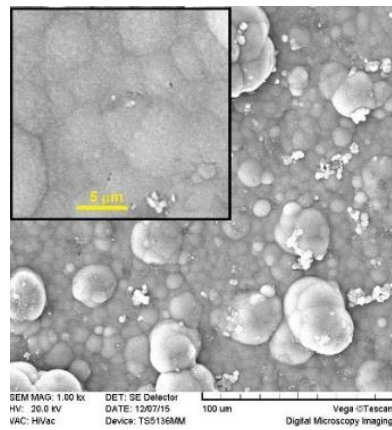
Fig. 3- Surface morphology of HA coating after one week soaking inside simulated body fluid.

Fig. 2- HRTEM image of the pulse deposited HA coating. Dash line indicates a nano-sized grain and arrows denote to irregular areas between adjacent grains.
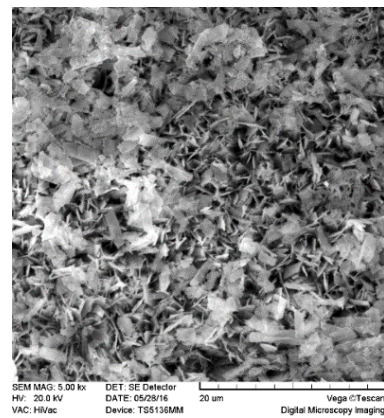
Fig. 4- Surface morphology of HA coating after contacting with an external body.

To apply a biodegradable polymer film on the coated alloy, the synthesis of mPEG-b-PCL diblock copolymers was carried out at the first step using ε-CL and mPEG (MW = 1000). The chemical structures of mPEG-*b*-PCL copolymers were characterized with ¹H NMR analysis and typical spectra was shown in Fig. 5.

The protons in the repeating units are assigned with numbers in the inset structure, and their corresponding peaks are indicated in the spectrum. In Figure 5, −OCH$_2$CH$_2$O− in the PEG part (proton-2) appeared at 3.65 ppm, and upon polymerization a new ester peak appeared at 4.05 ppm; all other CL repeating unit protons appeared with respect to the expected structure. The comparison of the peak intensities of the PEG part (proton-2 at 3.65 ppm) and the CL repeating units

(protons at 4.05 ppm) gave the number average degree of polymerization, n=96 in the present case (MW≈5000).

Fig 6a shows a polymer/ HA bilayer coating on Nitinol alloy confirming a uniform covering of the polymer film on the HA coating. This film improves the toughness of the HA coating as seen in Fig. 6b which is taken after the scratch test. It can be seen that the polymer film is stretched around the track as a result of the high scratching force; however the surrounding coating is remained attached to the substrate. So, it is concluded that the polymer film confines the possible damaged area on the HA coating.

One of the concerns of polymer coatings applications on implants is changing the biological condition at the interface of the implant and
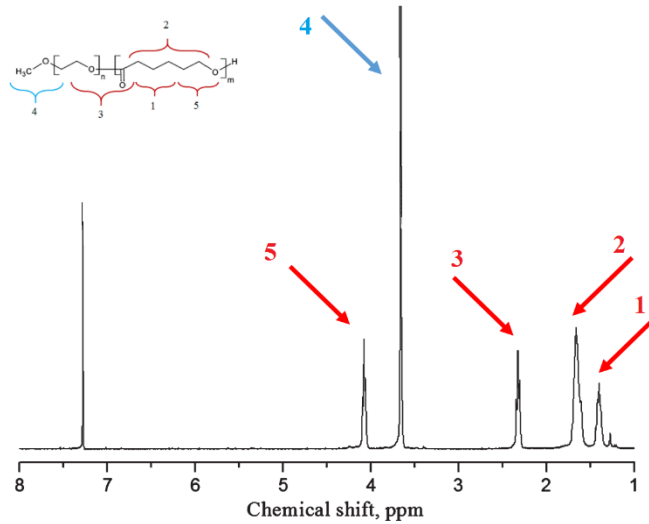
Fig. 5- 1H NMR spectrum of mPEG-b-PCL96.
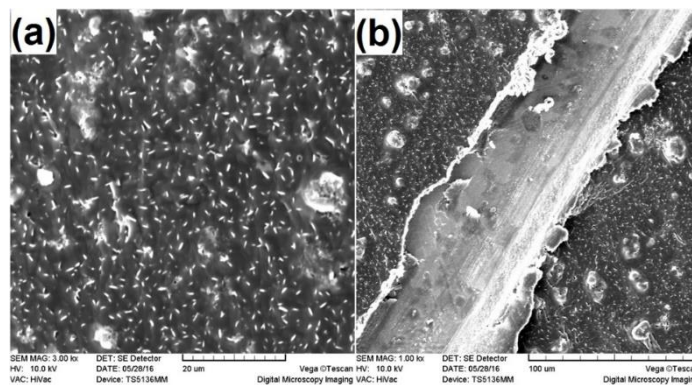
Fig. 6- (a) mPEG-b-PCL/hydroxyapatite bi-layer coating on Nitinol alloy revealing a uniform covering of polymer coating. (b) Scratch mark on the composite coating representing good adhesion strength of the coating to substrate.

biological mediums. It means that beside the positive effect of the polymer coating on toughening of the composite film, the bioactivity of the HA coating can be destroyed in this condition. It was shown that some biodegradable polymers like PLA release acidic products during degradation process. This can result in a drop of pH and dissolve the hydroxyapatite film [23]. However, in mPEG-*b*-PCL copolymer there were no dimer, trimer, or higher oligomers detected after the degradation and the amount of 6-hydroxyhexanoate remained at very low levels after several weeks [24].

As the polycaprolactone –polyethylene glycol copolymer is degraded by a hydrolytic process, the degradation effect of the polymer coating on HA film was examined by soaking the bilayer film inside phosphate buffered saline. Fig. 7a shows that after three days the beneath HA film is revealed without any considerable changes on morphology. This result show that copolymerization of PCL with PEG has been resulted in fast degradation of copolymer which offer the beneath layer to contact with the surrounding tissue after a short time. Also, high resolution images (Fig. 7b) reveals that some Ca-P compounds are formed during soaking the sample inside PBS as a result of the high bioactivity of coatings. This observation can show that the application of the biodegradable co-polymer coating guarantees both the toughness and the bioactivity of HA coating on Nitinol alloys. However, the best degradation time of the co-polymer film must be adjusted by modifying the structure of co-polymer. The details of these data will be reported in our future works.

4. Conclusions

Based on the results of this work, the bipolar pulsed electrodeposition process can produce nanostructured HA film on the Nitinol alloy with a uniform nanowall morphology. The plates of the coating contains nano sized grains and some irregular regions can be detected among the grains. New calcium-phosphate crystals (Ca/P=1.7) are rapidly formed on the nano-HA coating confirming the bioactive behavior of the sample. The mechanical weakness of the nano-sized crystals against external forces can be compensated by applying mPoly(Ethylene Glycol)-*b*-Poly(Caprolactone) film. mPEG-*b*-PCL can be degraded after a short time of implantation and reveals the beneath bioactive HA film without any damage on the coating.

Acknowledgments

References:
1. Pelton AR, Stöckel D, Duerig TW. Medical Uses of Nitinol. Materials Science Forum. 2000;327-328:63-70.
2. Elahinia MH, Hashemi M, Tabesh M, Bhaduri SB. Manufacturing and processing of NiTi implants: A review. Progress in Materials Science. 2012;57(5):911-46.
3. Tian H, Schryvers D, Liu D, Jiang Q, Van Humbeeck J. Stability of Ni in nitinol oxide surfaces. Acta Biomaterialia. 2011;7(2):892-9.
4. Espinar E, Llamas JM, Michiardi A, Ginebra MP, Gil FJ. Reduction of Ni release and improvement of the friction behaviour of NiTi orthodontic archwires by oxidation
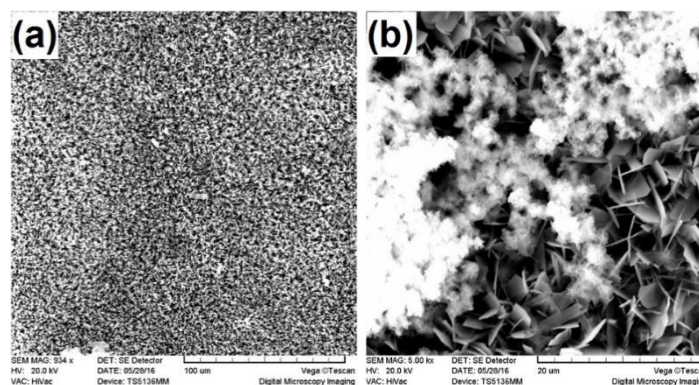
Fig. 7- (a) Surface morphology of the polymer coated HA film after degradation of the polymer during incubation inside PBS for three days. (b) High resolution image revealing precipitates that were formed after degradation of polymer inside PBS.

treatments. Journal of Materials Science: Materials in Medicine. 2011;22(5):1119-25.

5. Cui ZD, Chen MF, Zhang LY, Hu RX, Zhu SL, Yang XJ. Improving the biocompatibility of NiTi alloy by chemical treatments: An in vitro evaluation in 3T3 human fibroblast cell. Materials Science and Engineering: C. 2008;28(7):1117-22.

6. Campbell AA. Bioceramics for implant coatings. Materials Today. 2003;6(11):26-30.

7. Watabe N. Studies in shell formation. Crystal–matrix relation-ships in the inner layers of mollusk shells. Calcif Tissue Int. 1965;29:163–7.

8. Du C, Cui FZ, Feng QL, Zhu XD, de Groot K. Tissue response to nano-hydroxyapatite/collagen composite implants in marrow cavity. Journal of Biomedical Materials Research. 1998;42(4):540-8.

9. Kim H-W, Knowles JC, Kim H-E. Hydroxyapatite and gelatin composite foams processed via novel freeze-drying and crosslinking for use as temporary hard tissue scaffolds. Journal of Biomedical Materials Research Part A. 2004;72A(2):136-45.

10. Fratzl P, Gupta HS, Paschalis EP, Roschger P. Structure and mechanical quality of the collagen–mineral nano-composite in bone. J Mater Chem. 2004;14(14):2115-23.

11. Peter M, Ganesh N, Selvamurugan N, Nair SV, Furuike T, Tamura H, et al. Preparation and characterization of chitosan–gelatin/nanohydroxyapatite composite scaffolds for tissue engineering applications. Carbohydrate Polymers. 2010;80(3):687-94.

12. Kim H-W, Knowles JC, Kim H-E. Hydroxyapatite/poly(ε-caprolactone) composite coatings on hydroxyapatite porous bone scaffold for drug delivery. Biomaterials. 2004;25(7-8):1279-87.

13. Coombes AGA, Rizzi SC, Williamson M, Barralet JE, Downes S, Wallace WA. Precipitation casting of polycaprolactone for applications in tissue engineering and drug delivery. Biomaterials. 2004;25(2):315-25.

14. Oyane A, Kim H-M, Furuya T, Kokubo T, Miyazaki T, Nakamura T. Preparation and assessment of revised simulated body fluids. Journal of Biomedical Materials Research. 2003;65A(2):188-95.

15. Etminanfar MR, Khalil-Allafi J, Parsa AB. On the electrocrystallization of pure hydroxyapatite nanowalls on Nitinol alloy using a bipolar pulsed current. Journal of Alloys and Compounds. 2016;678:549-55.

16. Ikoma T, Yamazaki A, Nakamura S, Akao M. Preparation and Structure Refinement of Monoclinic Hydroxyapatite. Journal of Solid State Chemistry. 1999;144(2):272-6.

17. Elliott JC. Preface. Structure and Chemistry of the Apatites and Other Calcium Orthophosphates: Elsevier; 1994. p. v-vii.

18. Haverty D, Tofail SAM, Stanton KT, McMonagle JB. Structure and stability of hydroxyapatite: Density functional calculation and Rietveld analysis. Physical Review B. 2005;71(9).

19. Ikoma T, Yamazaki A, Nakamura S, Akao M. Preparation and Structure Refinement of Monoclinic Hydroxyapatite. Journal of Solid State Chemistry. 1999;144(2):272-6.

20. Hochrein O, Kniep R, Zahn D. Atomistic Simulation Study of the Order/Disorder (Monoclinic to Hexagonal) Phase Transition of Hydroxyapatite. Chemistry of Materials. 2005;17(8):1978-81.

21. Landolt D, Marlot A. Microstructure and composition of pulse-plated metals and alloys. Surface and Coatings Technology. 2003;169-170:8-13.

22. Zhu SL, Yang XJ, Cui ZD. Formation of Ca–P layer on the Ti-based bulk glassy alloy by chemical treatment. Journal of Alloys and Compounds. 2010;504:S168-S71.

23. Li S, Garreau H, Vert M. Structure-property relationships in the case of the degradation of massive poly(α-hydroxy acids) in aqueous media. Journal of Materials Science: Materials in Medicine. 1990;1(4):198-206.

24. Huang M-H, Li S, Hutmacher DW, Schantz J-T, Vacanti CA, Braud C, et al. Degradation and cell culture studies on block copolymers prepared by ring opening polymerization of ε-caprolactone in the presence of poly(ethylene glycol). Journal of Biomedical Materials Research. 2004;69A(3):417-27.